

Migration of THO & Np in a Fractured Granite Core at Deep Underground Laboratory

Chung-Kyun PARK *, Won-Zin CHO , Pil-Soo HAHN and B.KIENZLER
Korea Atomic Energy Research Institute, 150 Duck-Jin Dong, Yusung-Ku, Daejeon

ckpark@kaeri.re.kr

Abstract

Migration experiments of THO and ^{237}Np have performed through a sampled granite core in Chemlab2 probe at the Äspö hard Rock laboratory. The elution curves of THO were analysed to determine hydraulic properties such as the extent of dispersion effect according to flow rates. The retardation phenomena of the solutes were observed and described with elution curves and migration plumes. After migration test, the rock core was opened, and the remaining radioactivities on the rock fracture surfaces were measured. The transport process was simulated with a two-dimensional channel model. The mass transport process was described with three types of basic processes ; advection, sorption and matrix diffusion. By the combination of these processes, effects of each process on transport were described in terms of elution curves and migration plumes. By comparing the simulation results to the experimental one, it was possible to analyse the retardation effect quantitatively.

1.Introduction

Actinide elements show a very complex geochemical behaviour, which is influenced by changes of redox state of the nuclides, complexation with groundwater constituents and colloid formation. Sorption of actinides depends strongly on the actual speciation in the groundwater. Investigation of the sorption behaviour under the most realistic conditions attainable is required. A series of Actinide migration experiments have been conducted at the ÄspöHard Rock Laboratory(HRL) in Sweden. The HRL was established in a granite formation for in-situ test on disposal topics. To guarantee most realistic conditions, the experiments have been performed in the in situ CHEMLAB 2 probe. This work is one of the series experiments and described experimental results of sorption and migration for THO and ^{237}Np . Previous results of these kinds of experiments were reported [1,2].

The objectives of this study are as follows,

To investigate the applicability of retardation coefficient measured in batch test ,

To study the extent of matrix diffusion according to flow rates or contact times.

To validate migration processes by identifying the migration plumes between experiments and simulations for various cases, and

To study the applicability of the variable aperture channel model with the particle tracking method.

2. Experimental system

2.1 Groundwater and rocks

For the in situ experiments, the groundwater was connected directly from the CHEMLAB2 probe. The pH was 7.5 and DOC was 42.3mg/l for the water. The Eh values were varied

from +50 mV to -200 mV. Other properties of the groundwater was well described in the reference.[3] Granite cores were sampled at the boreholes in the Äspö HRL. Specific surface area of the grinded sample was about 1.1 m²/g by BET test. The fracture is several mm wide with different layers of K-feldspar, epidote/chlorite, Fe(III)oxide/hydroxide and calcite. Most of the surfaces seem to be covered with hydrothermally grown K-feldspar crystals or epidote but redistribution of quartz is associated with the hydrothermal alteration and it is possible that other parts of the fractures are coated with hydrothermally grown quartz crystals. The core was cut as the length of 150mm and the diameter of 52mm for the migration test.

2.2 Experimental system and procedures

The experimental setup was especially designed like an autoclave type reactor to endure high pressure conditions. A core sample having a single fracture was placed into a cylindrical stainless steel sleeves. The periphery was filled with epoxy resin. The leak tightness was up to 60 bar water pressure. While the water pressure in CHEMLAB2 is about 27 bar. The schematic diagram of the in-situ experimental setup was shown in Fig.1.

Before the in-situ experiment, the preliminary migration experiments using tritiated water (THO) were performed in a glove box under a 99% Ar & 1% CO₂ atmosphere in the laboratory. 0.01 bar of PCO₂ is exceeded the partial pressure at Chemlab2 site by about 10 times. On the other hand, a glove box was installed at the in-situ test site and equipped withan inert gas system restricting oxygen concentration to about 1 ppm. The autoclave was inserted into the drill hole, coupled to the glove box.

For the migration experiment, the actinide cocktail was prepared as described in Table 1 and injected for 10 days with a flow rate of 0.04 ml/h. Afterwards, natural groundwater of the drill hole was pumped. However, a technical problem caused fluctuations in the flow rate. Thus the test was interrupted after 45 days and the setup was fixed. The migration test was continued again at a higher flow rate of 0.3ml/h for 54 days. Afterwards, the core was recovered and opened.

Table. 1 Composition of the actinide cocktail of 50 ml used for the migration experiment

Nuclide	Activity of the cocktail (50 ml) <i>Bq / 50 ml</i>	Impurities <i>Bq / 50 ml</i>	Concentration <i>mol / L</i>
HTO	9x10 ³		
²³⁷ Np	3.3x10 ³		1.1x10 ⁻⁵
²⁴² Pu	1.7x10 ²	²³⁸ Pu: 38 ²³⁹ Pu: 15	9.7x10 ⁻⁸
²⁴³ Am	8.0x10 ²	^{243/244} Cm: 1.5x10 ³	8.9x10 ⁻⁹

3. Characterization of the aperture and Hydraulic properties

In order to map the aperture distribution in the fracture core, the optical images of the rock slices and the images of X-ray tomography were analysed. The fracture of the core was described as a two dimensional geometric field in the simulation with a variable aperture

channel model. The fracture field was divided by 20 (in the fracture plane) x 31 (in the direction of flow) subsquares reflecting its geometry ; the diameter of 5.2 cm and the length of 15cm. From the scanning image of the fracture at each slice, the aperture value at each subsquare point was calculated. A two dimensional distribution of the aperture in the whole fracture plane was obtained by the Krigging method and plotted with the graphic software, Surfer in Fig.2. The top figure shows a three dimensional contour of the aperture distribution in the fracture and the bottom plane was described as a flat one to figure out the aperture height easily. The plot of z- axis describing aperture values is exaggerated also for easy showing. The middle figure shows two dimensional contour map of the same aperture distribution. The fracture field is well developed and there is no local closed zone except both edges of the inlet face. By summing up the aperture value at each point, the pore volume in the fracture space was obtained as 2.33 cm³. And the mean aperture value was calculated 0.031 cm by dividing the pore volume with the geometric surface area of the fracture plane.

The flow system in the core was assumed as a line source-in and a line flow-out system, that is, a line source solution contacts on the surface boundary of the rock core and flow out the opposite side of the fracture boundary. A governing equation and boundary conditions were set for the flow system consisted of 20*31 subsquares like the finite different meshes. The fluid flow through the fracture was then calculated for a constant flow rate as well as for constant pressure conditions. The volumetric flow rate, Q_{ij} , at a subsquare may be written as:

$$Q_{ij} = C_{ij} (P_i - P_j) \quad (1)$$

where P_i is the pressure at node i, Node i implies an index of the ith subsquare in the fracture surface. C_{ij} is the flow conductance between nodes i and j. The mass balance at each node may be written as:

$$\sum_j Q_{ij} = \sum_j C_{ij} (P_i - P_j) = E_i \quad (2)$$

where E_i is the injection rate or elution rate at node i. The subscript j stands for the four facing nodes of surrounding subsquares to node i. By rearranging the above equation for each node, it can be obtained a system of linear equations in the form,

$$[B] [P] = [E] \quad (3)$$

where [B] is a coefficient matrix describing the flow conductance. The matrix [P] is an array describing the pressure distribution and [E] is an array describing net flow rates. Except for the nodes at the boundaries, the pressure at each node can be solved an iteration method. The flow between adjacent nodes can be calculated using equation (2). After obtaining flow vectors at all nodes, solute transport can be simulated in this flow field.

The simulated pressure distributions in the fracture were shown at the bottom figure in Fig.2. The pressure drop between the inlet and the outlet is about 24 dyne/cm² when flow rate is 0.04 ml/h. That is, there is only a little pressure drop along the main flow field. The pressure drop at the both edges in the inlet side having very small aperture can be ignored

because it gives little effects on the flow. The pressure drop in the CHEMLAB was measured less than 0.1 bar (~ 105 dyne/cm²) at the sample, which not only over the fracture but also over a 17-20m long 1/16" tube line. The distribution of the pressure shows almost symmetric to the center line of the fracture plane along the longitudinal axes.

4. Migration of the Radionuclides

A two-dimensional random-walk particle tracking algorithm was used to simulate the solute transport through the flow fields. Four transport processes were considered : advection, longitudinal dispersion, diffusion into the rock mass, and sorption. Particle displacements in each time step consisted of an advective displacement based on local velocities calculated using the pressure field, random diffusive displacement, and retardation by sorption. Particles, which are representing the mass of a solute contained in a defined volume of fluid, move through a fracture with two types of motion. One motion is with the mean flow along stream lines and the other is random motion, governed by scaled probability for matrix diffusion and sorption[Washburn,1980]. At the inlet, a certain amount of particles were introduced and distributed at each node between flow channels with a probability proportional to the flow rates. Particles are then advected and retarded by discrete steps from node to node until they reach the outlet node at which point the arrival time is recorded. This procedure is repeated for all the particles to get a stable probability distribution which in turn can be regarded as an elution concentration. The residence time of a particle along each path is obtained as the sum of the residence times in all subsquares through which the particle had passed. The migration plum can be obtained by checking the positions of the particles in the fracture surfaces at a certain time.

4.1 Transport of conservative tracer

The HTO elution curves according to various flow rates in the lab. experiment are shown in Fig.3. The hydraulic properties of the curves were arranged in Table 2. All three experiments were measured by means of a flow through detector. Thus, it has a certain uncertainty in quantifying sample volume because of the residence time of the solution in the detector and the continuous measurements. In order to analyse the elution curves quantitatively, the curves were normalized by summing up the eluted concentrations and volumes. And recovery percentages are assumed as 100 % or 80 % in order to the experimental uncertainty.

Two transport cases are considered in the simulation ; in the first case (S1), tritium transports only by advection along the flow field, and in the other case(S2), the tracer migrates by advection and diffusion through the pores of the fracture surface. The proposed pore diffusivity is $1.5 \cdot 10^{-10}$ m²/s. [4] For this case, the formation factor, f , has about 0.06 , while it has a value in the range of 0.01 ~ 0.4 in rocks. In this paper it was not tried to get the optimum value of the diffusivity but choose a reasonable value as a measure of comparison.

The normalized experimental and the simulated curves were plotted together in Fig.3. There is no significant difference among the three experimental curves in this flow range. The jumped base lines of the experimental data at the early stages of the elution seems due to remaining tail of previous experiments. In order to check the degree of the matrix diffusion, a theoretical response function (S3) was plotted with the experimental curve (E1) of $Q=0.26$ ml/h. The S3 was assumed a pulse injection and unlimited matrix diffusion. Hadermann[5]

suggested that the S3 has a functional form as

$$C/C_0 = \text{Const} * t^{-3/2} \tag{4}$$

The S2 shows similar slope to the S3. It means they have same migration trend in spite of their different system conditions. The three experimental curves also approaches to the S2. Thus, it is reasonable assumption that THO diffuses into the rock pore during transporting on the fracture in these flow rates. The fast flow curves, E1 and E2, show a little sharper slope than that of S3, while the slowest curve of $Q=0.282\text{ml/h}$, E3, approach to the slope of S3. It implies when the flow is slow, there is much chance to diffuse into the rock pore, Therefore, the in-situ test, the flow rate of 0.04ml/h , will be given later, may show larger diffusion effect than E3.

The concentrations of the elution curves are summed up with time and plotted as cumulative elution curves as a function of the eluted volume. Because the recovery percentages of the three experiments were not clear, it was simulated its recovery as 80% or 100 % and shown in Fig.8 and 9, respectively. Though the deviation between the experimental and S2 curves in the case of 100 % recovery in Fig.4 is larger than that of 80 %, the slopes of the experimental curves are more similar to 100% case than that to 80%. When the tail and perturbation effects of previous experiments are compensated in the early elution stages, The experimental curves may approach closer to the S2 curve. And it implies that recovery percentage of THO is larger than 80% and close to 100 % in these experiments.

Table 2 Hydraulic properties of the migration system

Flow rate		6.36 ml/h	2.82 ml/h	0.282 ml/h
l	m	0.15	0.15	0.15
t_0	s	1448323	3954919	300976840
v_0	m/s	$(1.040.23) \times 10^{-4}$	$(3.790.88) \times 10^{-5}$	$(5.011.14) \times 10^{-6}$
σ_t^2	-	1.090	1.088	1.12
D	m^2/s	8.48×10^{-6}	3.07×10^{-6}	4.19×10^{-7}
a	m	8.17×10^{-2}	8.08×10^{-2}	8.36×10^{-2}
Pore Volume	ml	2.60.6	2.70.6	2.3 0.5
Porosity	%	0.82	0.85	0.72
Peclet Number	-	1.84	1.54	1.79

The elution curve of THO in the in-situ experiment is shown in Fig.5. It shows somewhat different characteristics comparing to the lab. tests. It may due to the different experimental environment between two systems. The experimental curve was normalized using above assumptions and shown as a function of the eluted volume. The transport of THO in the in-situ condition was also simulated with the flow rate of 0.04 ml/h and pore diffusivity of $1.5 \times 10^{-10} \text{ m}^2/\text{s}$. The simulated elution and cumulative curves are also shown together in Fig.5. The simulated curves match each other with the experimental ones reasonably.

4.2 The migration of ^{237}Np

remaining concentration of ^{237}Np in the fracture after migration test is determined by γ -counting and dissolution of the slice. And an average concentration profile over the whole fracture is shown in Fig.6. This profile was obtained by taking into account that in total eluted water was about 210 ml. From the profile the retardation factor, R_s , is determined using eq.(1) as 243.

$$R_s = \frac{V_w}{V_n} = \frac{\ell_w}{\ell_n} = \frac{Vol}{S_a \cdot \ell_n} \quad (5)$$

Where V is flow velocity, ℓ is migration length, Vol is eluted volume of the solution, S_a surface area of the fracture, subscript w & n are water and nuclides, respectively.

In order to simulate the migration plumes of ^{237}Np , the following four cases were considered as summarized in the Table 2. The simulation was carried out with the particle tracking method when the water flow rate was 0.04 ml/h and shown as three dimensional plumes as a function of eluted volume[6].

Table 2 Simulation of the migration for sorbing tracers

	Retardation factor, R_s	Pore Diffusivity D_p (m^2/s)	Remarks
Case 1	69	-	Elution peak around 50 ml
Case 2	69	$1.5 \cdot 10^{-10}$	Eluted from 100 ml Widely dispersed
Case 3	243	-	Elution peak around 80 ml
Case 4	243	$1.5 \cdot 10^{-10}$	Similar profile as the experimental
THO	-	$1.5 \cdot 10^{-10}$	Elution peak around 20 ml

In the first case, the radionuclide retards only by sorption with $R_s = 69$. The nuclides flow out almost when the water eluted about 50 ml. The case 2 is added the matrix-diffusion process from the case 1. The proposed pore diffusivity is $1.5 \cdot 10^{-10} \text{ m}^2/\text{s}$ as same as the tritium. It shows much retarding effect than the case 1. The nuclide starts to come out from the water elution volume of 100ml. In the case 3, the radionuclide retards only by sorption as the case 1 but $R_s = 243$. The main migration plume comes out when the water eluted about 80 ml. The case 4 is added the matrix diffusion process from the case 3. It shows much retarding effect than the case 3. Its migration plume at 210 ml of the eluted volume shows very similar profile with the experimental one as shown in Fig.7. Thus matrix diffusion process gives a significant retardation and dispersion effect in the migration process comparing to the case of sorption only in this flow system. Therefore, when $R_s = 243$ and the pore diffusivity is $1.5 \cdot 10^{-10} \text{ m}^2/\text{s}$. The migration plume fits very well to the experimental result.

5.2.2 Comparison to sorption behavior determined in batch tests

Following relation can be obtained for the retardation coefficient R_s :

Following relation can be obtained for the retardation coefficient R_s :

$$R_s = \frac{\text{mass}_{\text{sorbed}}}{\text{mass}_{\text{dissolved}}} = \frac{c_0 \cdot K_s \cdot \text{surface}_{\text{fracture}}}{c_0 \cdot \text{volume}_{\text{fracture}}} = \frac{K_s \cdot f}{\delta} \quad (6)$$

where, C_0 : dissolved concentration, K_s : distribution coefficient based surface area, f : form factor for surface area, δ : aperture of the fracture

The form factor for surface area includes deviations of the actual surface and void volume of the fracture from the calculated geometrical properties. Combining the Np sorption data with the information obtained from sorbed Np in the core, a form factor for the surface of 21.5 is calculated. From the batch K_s data, R_s value of ^{237}Np can also be obtained. It is very interesting topic to compare the values secured from the static batch and the dynamic migration test. If the determined values are adopted from eq.(2), such as $K_s = 0.16\text{cm}$ and $f = 21.5$, and $\delta = 0.031\text{ cm}$, then R_s of ^{237}Np is calculated as 111, which is lower value than the value of 243 obtained from the migration simulation. It may be caused by the difference of contacting time. In the batch test, radionuclides were contacted for 14 days. While in the migration test, they were contacted more than 50 days. The longer contact time gives much chance to diffuse into the pore and to sorb. Thus it will give larger value of R_s than 111. That is, $R_s = 243$ from the migration is seemed as a reasonable value.

Conclusion

The migration of ^{237}Np through a fractured granite core at in-situ condition showed much retarded effect than expected from the static sorption test. It is interpreted due to difference of the contact time between nuclides and rock fracture. That is, much contact time in migration test shows much retarding phenomena than the batch test. The developed variable aperture channel model was successfully applied in describing the migration of radionuclides in the rock fracture. Results from the migration test and modelling of the transport show that diffusion into the interconnected micropore space in the rock mass has an effect on the retardation, especially for the case of tritium and ^{237}Np .

References

1. B.Kinzler, P.Vejmelka, Römer, J., Fanghänel, Th., P.Wilberg, M.Jansson, T.Eriksen ; Swedish-German actinide migration experiment at ÄSPÖ HRL. , 8th Internat.Conf.on Chemistry and Migration Behaviour of Actinides and Fission Products in the Geosphere (Migration '01), Bregenz, A, September 16-21, 2001, Journal of Contaminant Hydrology 61 (2003) 219- 233
2. J.Römer, Kienzler, B., Vejmekla, P. E.Soballa, A.Gortzen, M.Fuss, Actinide migration experiment in the HRL ÄSPÖ, Sweden: results of laboratory and in situ experiments (Part II). Wissenschaftliche Berichte, FZKA-6770 (Oktober 2002)
3. Moreno L. and Neretnieks I., Flow and nuclide transport in fractured media, J. of Cont. Hydrol. 13 (1993), 49-71
3. P.Vejmelka, Fanghänel, Th., Kienzler, B., Korthaus, E., Römer, J., Schüßler, W., Artinger, R., 2000. Sorption and migration of radionuclides in granite (HRL ÄSPÖ, Sweden). For-schungszentrum Karlsruhe, FZKA 6488.

4. C.K.Park, T. T. Vandergraaf, D. J. Drew, and Hahn, P.S., Analysis of the Migration of nonsorbing tracers in a natural fractures in granite using a variable aperture channel model, J. of Cont. Hydrol.26, 97 (1997).
5. J.Hadermann, The Grimsel Migration experiment : integrating field experiments, laboratory nvestigations and modelling, J. of Cont. Hydrol. 21 (1996) 87-100
6. C.K.Park, Ryu,B.H., and Hahn, P.S., Migration characteristics of some chemical species in a granite fracture according totheir chemical properties, Kor. J. of Chem. Eng., 19(5) 765 (2002)

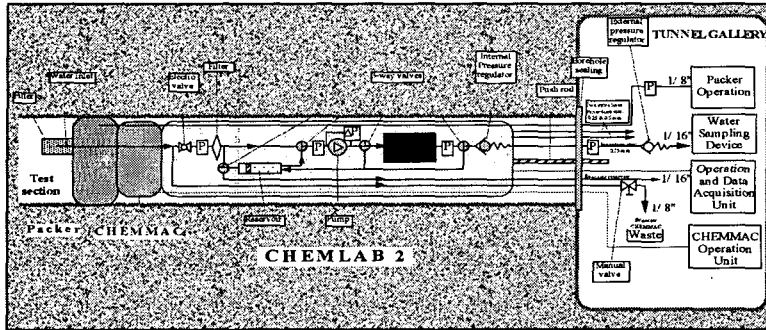


Fig. 1. in-situ experimental setup.

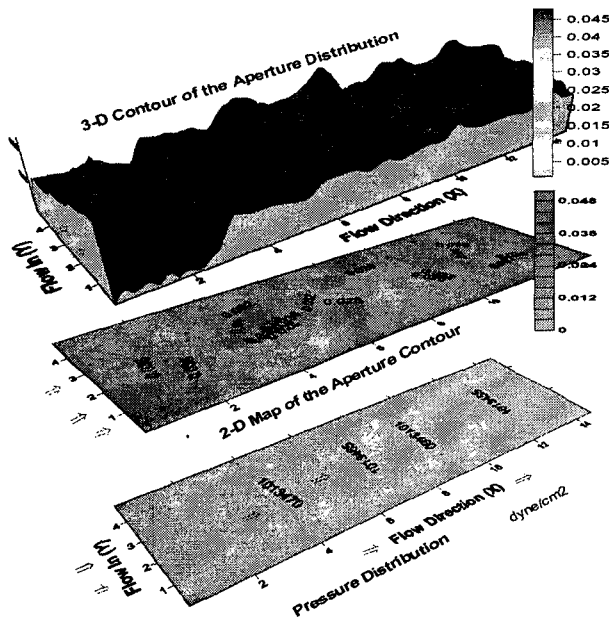


Fig.2 Aperture distribution of the granite core. Z axis is exaggerated for easy showing $\Delta P = 24$ dynes/cm² between inlet and outlet through the main stream

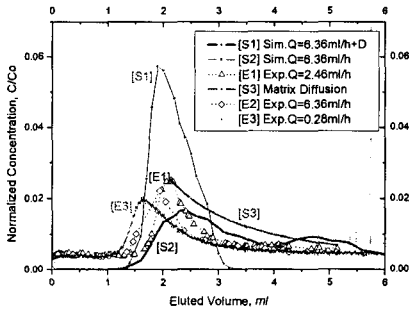


Fig. 3. Comparison of the elution curves of tritium to the simulated

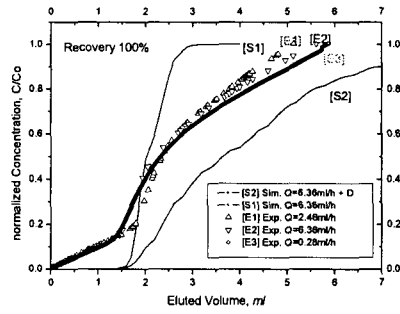


Fig. 4. Cumulative elution curves of tritium when the recovery is 100%.

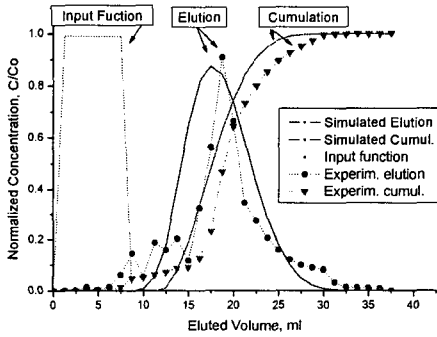


Fig. 5. Comparison of the in-situ elution curves to the simulated

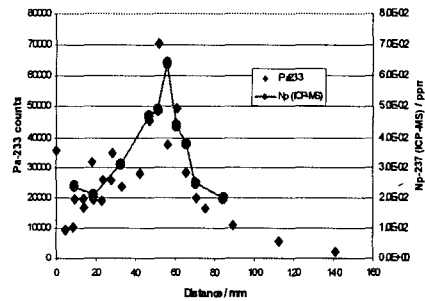


Fig.6. One dimensional Concentration profiles of nuclides in the fracture

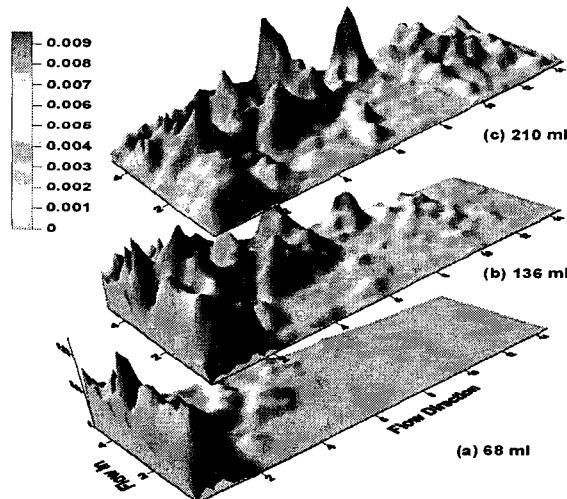


Fig.7 Simulation of the migration plumes of ^{237}Np with the eluted volume when $R_s = 243$ with diffusion